The Conserved C-Terminus of the Citrate (CitP) and Malate (MleP) Transporters of Lactic Acid Bacteria Is Involved in Substrate Recognition†

Michael Bandell and Juke S. Lolkema*

Department of Microbiology, Groningen Biomolecular Sciences and Biotechnology Institute, University of Groningen, Haren, The Netherlands

Received May 25, 2000; Revised Manuscript Received August 1, 2000

ABSTRACT: The membrane potential-generating transporters CitP of *Leuconostoc mesenteroides* and MleP of *Lactococcus lactis* are homologous proteins with 48% identical residues that catalyze citrate−lactate and malate−lactate exchange, respectively. The two transporters are highly specific for substrates containing a 2-hydroxycarboxylate motif (HO-CR_2-COO^-) in which substitutions of the R groups are tolerated well. Differences in substrate specificity between MleP and CitP are based on subtle changes in the interaction of the protein with the R groups affecting both binding and translocation properties. The conserved, 46-residue long C-terminal region of the transporters containing the C-terminal putative transmembrane segment XI was investigated for its role in substrate recognition by constructing chimeric transporters. Replacement of the C-terminal region of MleP with that of CitP and vice versa did not alter the exchange kinetics with the substrates malate and citrate, indicating that the main interactions between the proteins and di- and tricarboxylate substrates were not altered. In contrast, the interaction of the proteins with the monocarboxylate substrates mandelate and 2-hydroxyisovalerate changed in a complementary manner. The affinity of CitP for the *S*-enantiomers of these substrates was at least 1 order of magnitude lower than observed for MleP. Introduction of the C-terminal residues of MleP in CitP resulted in a higher affinity and vice versa. Interchanging the C-termini had a more complicated effect on the *R*-enantiomers, affecting different kinetic parameters with different substrates, indicating multiple interactions of the R groups at this side of the binding pocket. It is suggested that the binding pocket is located between transmembrane segment XI and the other transmembrane segments of the transporters.

The homologous citrate and malate transporters CitP and MleP found in the lactic acid bacteria *Leuconostoc mesenteroides* (*1*, *2*) and *Lactococcus lactis* (*3*, *4*) function in secondary metabolic energy-generating pathways. The transporters catalyze the uptake of a substrate into the cell coupled to the exit of a metabolic end product (precursor−product exchange; for a review, see ref *5*). CitP exchanges divalent citrate and MleP divalent malate for monovalent lactate, an end product of both citrate and malate degradation in lactic acid bacteria (*4*, *6*). Net charge movement over the membrane during exchange results in a membrane potential of physiological polarity. This, in combination with the generation of a pH gradient across the membrane due to the consumption of a cytoplasmic proton during the breakdown of citrate and malate, results in a proton motive force, and thus, the pathways generate metabolic energy for the cell. More recently, the pathways have been implicated in the recovery from acidic stress and resistance against lactate toxicity (*7*).

The substrates of CitP and MleP are structurally related (see Figure 1). The ability to exchange citrate or malate for lactate is associated with a high specificity for the 2-hydroxycarboxylate motif present in the substrates, i.e., HO-CR_2-COO^-, together with a low specificity for the two R groups (*3*). Next to the physiological substrates, CitP and MleP translocate a wide range of 2-hydroxycarboxylates with R groups ranging from hydrogen atoms in glycolate to a phenyl group in mandelate (*3*). A detailed kinetic analysis of the two transporters with different substrates showed that interactions with the OH and COO^- groups of the motif are essential for binding. The interactions with the two R groups (defined as R_R and R_S; see Figure 1) are not essential but modulate affinity and translocation efficiency (*8*). The tolerance toward the R groups gives the transporters their membrane potential-generating capacity. Two types of interactions take place between the R groups and the binding sites of CitP and MleP, depending on the nature of the R group (*8*). A strong, possibly electrostatic interaction results in high affinity for 2-hydroxycarboxylates bearing an additional carboxylate group at R_S (see Figure 1). For example, the *S*-enantiomer of malate is a high-affinity substrate. Noncharged R groups have a less strong, most likely hydrophobic interaction with the binding site, resulting in low affinity for monocarboxylates, like lactate.

The difference in substrate recognition by CitP and MleP is caused by subtle differences in the interactions with the R groups of the substrates. Most prominent are (i) the difference in affinity between the mono- and dicarboxylates which is 1 order of magnitude higher for CitP than for MleP and (ii) CitP is more promiscuous in the translocation step toward larger R groups than MleP. The latter feature is

† This work was supported by a grant from the Netherlands Organization for Scientific Research (NWO-CW).

* To whom correspondence should be addressed: Department of Microbiology, University of Groningen, Biological Centre, Kerklaan 30, 9751 NN Haren, The Netherlands. Phone: 31-50-3632155. Fax: 31-50-3632154. E-mail: j.s.lolkema@biol.rug.nl.

10.1021/bi0011882 CCC: $19.00
Published on Web 09/29/2000

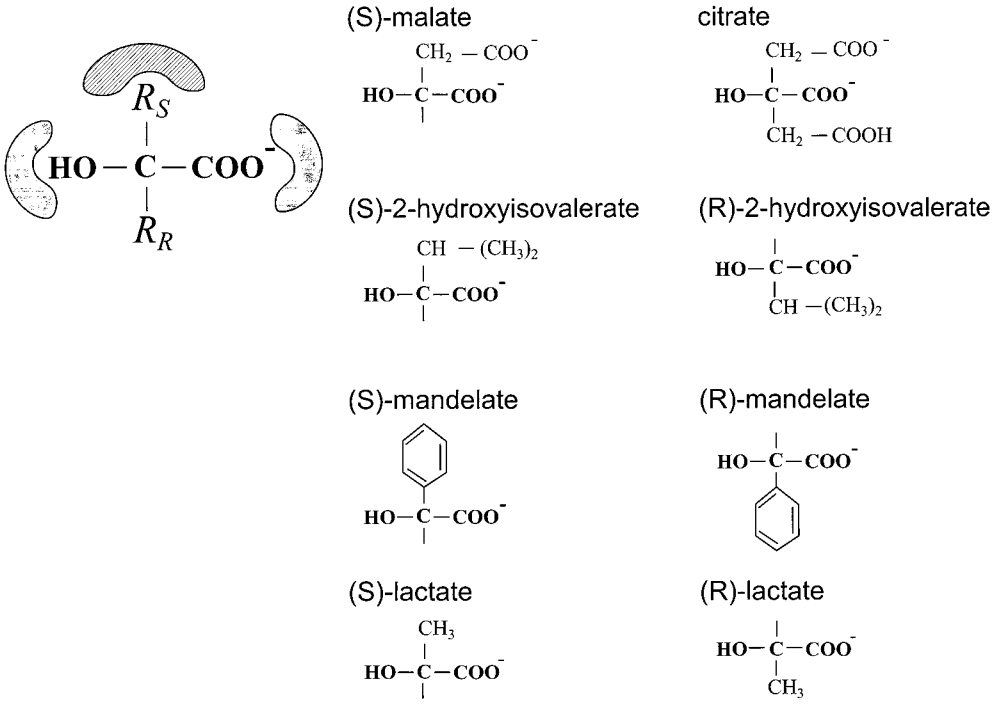

FIGURE 1: Model of the substrate binding site and structure of substrates of CitP and MleP. Sites on the proteins interacting with the essential OH and COO^- groups of the 2-hydroxycarboxylate motif are depicted as gray surfaces. The interaction site responsible for high-affinity binding of di- and tricarboxylates is depicted as a hatched surface. The two R groups are termed R_R and R_S according to the position of the R group in the *R*- and *S*-enantiomers of monosubstituted 2-hydroxycarboxylates (HO-CHR-COO^-), respectively. At the right are chemical structures of the substrates used in this study: malate, citrate, lactate, mandelate, and 2-hydroxyisovalerate. The 2-hydroxycarboxylate motif is bold.

responsible for the physiological function of the two transporters as citrate and malate transporters; CitP translocates both citrate and malate, while MleP translocates malate but cannot translocate the larger citrate molecule.

CitP and MleP are 48% identical in their amino acid sequences and belong to the 2-hydroxycarboxylate transporter (2-HCT)[1] family (*3*). The membrane topology model of these transporters consists of 11 transmembrane segments (TMS), based upon studies of the citrate transporter CitS of *Klebsiella pneumoniae*, which also belongs to the 2-HCT family (*9*−*11*). The C-terminal part of the amino acid sequences of the members of the 2-HCT family, including TMS XI and part of the cytoplasmic loop between TMS X and XI, is particularly well conserved. Since the main interactions with the substrates are very similar for CitP and MleP (*8*), this suggests that structural elements involved in substrate binding may be located in this part of the proteins (*3*). In the study presented here, we have constructed chimeric CitP−MleP transporters in which the conserved C-terminal parts of the proteins were interchanged. The chimeras were analyzed for their catalytic properties with 2-hydroxycarboxylate substrates bearing different R groups to locate the interactions between the proteins and the functional groups of the substrates in the C- or N-terminal part of the chimeras. The results suggest that the 46 C-terminal residues of MleP and CitP contain structural elements that interact with the R groups of the substrates.

[1] Abbreviations: 2HCT, 2-hydroxycarboxylate transporter; RSO, right-side-out; TMS, transmembrane segment; OD_{660}, optical density at 660 nm; PCR, polymerase chain reaction; SDS−PAGE, sodium dodecyl sulfate−polyacrylamide gel electrophoresis.

EXPERIMENTAL PROCEDURES

Bacterial Strains and Growth Conditions. L. lactis strain NZ9000 is a MG1363 derivative (*pepN*::*nisRnisK*; *12*) that transports neither citrate nor malate. The *nisR* and *nisK* genes were inserted into the chromosome to allow induced expression of plasmid-encoded citrate and malate transporters under control of the tightly regulated *nisA* promoter (*12*). Cells were grown at 30 °C in closed serum bottles and without shaking. The growth medium contained M17 broth (Difco) supplemented with 0.5% (w/v) glucose and 5 μg/mL chloramphenicol. Cells were induced by adding supernatant of the nisin-producing *L. lactis* strain NZ9700 (*13*), containing approximately 10 ng of nisin A/mL (*14*), to the cultures at an OD_{660} of 0.6. Typically, a 1000-fold dillution of the supernatant was added after which growth was continued for 1 h followed by harvesting of the cells by centrifugation. In some cases, a lower level of induction was used to allow kinetic analysis (see the Results). Then, cells expressing CitP, MleP, and MC397 were grown in the presence of a 30000-, 50000-, and 30000-fold dillution of the nisin-containing supernatant, respectively, for 0.5 h.

Construction of Expression Vectors and Chimeras. General procedures for cloning and DNA manipulations were performed essentially as described by Sambrook et al. (*15*). Ligation mixtures were transformed to *L. lactis* NZ9000 using an electroporation protocol described by Holo and Nes (*16*). Expression vector pGltThis (*17*) encodes the glutamate transporter of *Bacillus stearothermophilus*, with an N-terminal extension of six histidine residues (His tag) followed by an enterokinase proteolytic cleavage site. The coding region was amplified by the polymerase chain reaction

technique (PCR) using a forward primer (5′-ATTT**ACATGT**CGCATCACCATCACCATCACCATCACCATCACG-3′), containing an *Afl*III restriction site (bold) and 10 histidine codons (underlined), and a reverse primer downstream of the stop codon, containing an *Xba*I site (*17*). The *Afl*III−*Xba*I-digested PCR product was ligated into the *Nco*I−*Xba*I sites of the nisin inducible expression vector pNZ8048 (Cm^R, pSH71 replicon, inducible *nisA* promoter; O. Kuipers, unpublished), yielding pNZ*gltT*. Successful ligation destroys the *Nco*I site at this position. Subsequently, the *gltT* gene was removed, using the *Nco*I site just downstream of the enterokinase site (*15*) and the *Xba*I site downstream of the stop codon, and replaced with the *citP* and *mleP* genes containing *Nco*I−*Xba*I fragments from plasmids pMB*citP* and pMB*mleP* that were described previously (*3*). The resulting expression vectors, pNZ*citP* and pNZ*mleP*, encode the CitP and MleP transporter, respectively, extended with a 10-His tag and an enterokinase site at the N-terminus. The amino acid sequences of the N-terminal parts of CitP and MleP were MSHHHHHHHHHHDDDDKA**M**V**NHP**... and MSHHHHHHHHHHDDDDKA**M**GK**KLK**..., respectively, in which original residues are bold and the enterokinase site is underlined.

Chimeric transporters were constructed in two steps by overlap extension PCR (*18*) using the pNZ*mleP* and pNZ*citP* vectors as templates. The PCR products encoding the chimeric proteins were cloned into the *Nco*I−*Xba*I sites of pNZ8048 in the same way as described above for the wild-type genes. All constructs were verified by nucleotide sequencing.

Preparation of Membrane Vesicles and Exchange and Counterflow Assays. L. lactis NZ9000 cells expressing wild-type or chimeric transporters were cooled on ice and washed twice with 50 mM potassium phosphate (pH 6). Right-side-out (RSO) membrane vesicles were prepared by the osmotic shock lysis procedure essentially as described previously (*8*). Membrane vesicles were washed once in 50 mM potassium phosphate (pH 6) containing 5 mM (*S*)-malate and concentrated by centrifugation for 15 min in an Eppendorf tabletop centrifuge operated at full speed, followed by resuspension in the same buffer. For exchange measurements, the internal pool of (*S*)-malate was labeled with (*S*)-[^{14}C]malate by incubating the concentrated membranes with 186.7 μM L-[1,4(2,3)^{14}C]malate for 1 h at room temperature in the presence of 100 μM valinomycin and 50 μM nigericin. Aliquots (2 μL) were diluted into 200 μL of 50 mM potassium phosphate (pH 6) containing various substrates at the indicated concentrations and at 20 °C. For counterflow experiments, the (*S*)-malate-loaded concentrated vesicles were diluted 100-fold into 200 μL of buffer containing 9.8 μM L-[1,4(2,3)^{14}C]malate and different concentrations of various substrates when indicated. Final membrane protein concentrations in the assays were between 250 and 350 μg/mL. Reactions were stopped at the indicated times by addition of 4 mL of ice-cold 0.1 M LiCl, followed by rapid filtration over 0.45 μm pore size cellulose nitrate filters (Schleicher & Schuell). The filters were rinsed once with buffer and transferred to scintillation vials to determine the amount of retained radioactivity. Protein concentrations were determined as described by Lowry et al. (*19*).

Evaluation of the Data. Initial rates of exchange were determined by fitting the data to an exponential decay as described previously (*3*) using nonlinear fitting procedures provided with Sigma Plot (Jandel Scientific, San Rafael, CA). Exchange rates were determined at different external substrate concentrations. The affinity constant (K_m) for the substrate was determined by fitting the data to an equation describing competitive inhibition that takes into account the concentration of (*S*)-[^{14}C]malate in the external buffer caused by the dilution of the (*S*)-malate-loaded vesicles (see ref *8*). Initial rates of counterflow were estimated from internalized label measured in triplicate at 2 and 4 s. Data were used only when the rate of uptake increased in proportion with time to ensure initial rate conditions. Inhibition of (*S*)-malate counterflow by a substrate was assessed at different concentrations of the substrate in the external buffer. The inhibition constant (K_i) for the substrate was estimated as described previously (*8*) by fitting the data to an equation describing competitive inhibition. When the affinity for the substrate was low, K_i values were estimated from a single concentration of 20 mM measured at least in triplicate. A lower limit for the K_i was calculated when the extent of inhibition was less than 10%. A K_m for exchange or a K_i for counterflow was determined, depending on the transport properties of the substrate (*8*).

SDS−PAGE and Immunoblot Analysis. Right-side-out membrane vesicles (15 μg of protein/lane) were subjected to SDS−PAGE using a 12% polyacrylamide gel matrix. Following electrophoresis, the proteins were transferred to poly(vinylidene difluoride) membranes and analyzed using monoclonal antibodies directed against a His tag (Dianova, Hamburg, Germany). Antibodies were visualized using the Western-light chemiluminesence detection kit (Trophix, Bedford, MA).

Materials. L-[1,4(2,3)-^{14}C]Malic acid (51 mCi/mmol) and [1,5-^{14}C]citric acid (115 mCi/mmol) were obtained from Amersham International (Buckinghamshire, U.K.). All other compounds were obtained from Fluca (Buchs, Switzerland) or Sigma (St. Louis, MO).

RESULTS

Construction of Chimeric Transporters. Figure 2 shows a multiple-sequence alignment of the C-terminal part of the members of the 2-hydroxycarboxylate transporter family together with a topology model. To evaluate the involvement of the conserved C-terminal part of the CitP and MleP transporters in substrate binding, four chimeric transporters (CM397, CM353, MC397, and MC353) were constructed. Capitals indicate the origin of the N- and C-terminal parts of the chimera (C for CitP and M for MleP), and the number indicates the position of the amino acid residue preceding the junction (CitP numbering). Thus, CM397 consists of the 397 N-terminal residues of CitP and the 46 C-terminal residues of MleP, whereas the complementary chimera MC397 consists of the corresponding N-terminal part of MleP followed by the C-terminal residues of CitP. Wild-type and chimeric transporters were expressed in *L. lactis* NZ9000 cells under control of the inducible *nisA* promoter (*12*). The expression vectors differed only in the coding sequences of the transporter proteins. Wild-type and chimeric transporters were tagged with 10 histidine residues at the N-terminus to allow analysis of expression levels (see Experimental Procedures).

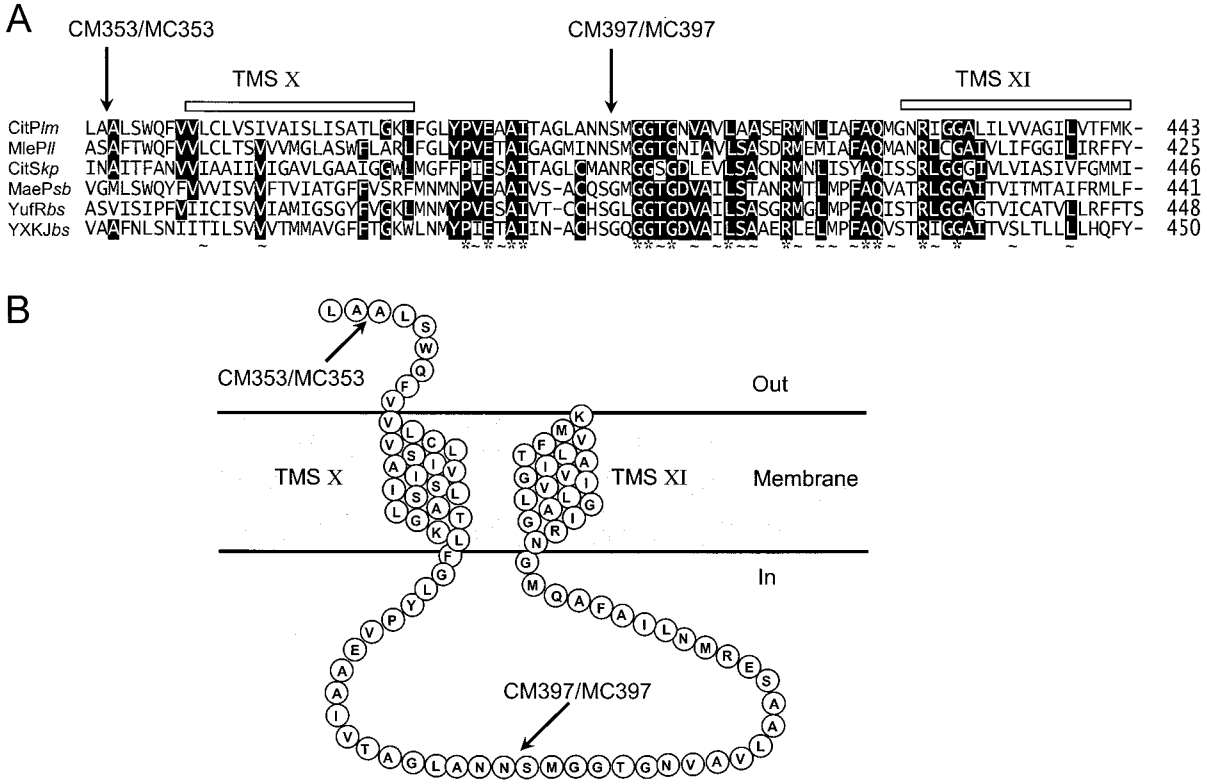

FIGURE 2: Amino acid sequence alignment (A) and topology model (B) of the C-terminal part of representative members of the 2-HCT family. (A) Transporters included in the alignment were the citrate transporter of *L. mesenteroides* CitP*lm* (*2*), the malate transporter of *L. lactis* MleP*ll* (*3*), the citrate transporter of *K. pneumoniae* CitS*kp* (*23*), the malate transporter of *Streptococcus bovis* MalP*sb* (*24*), and two open reading frames found on the *Bacillus subtilis* chromosome, YufR*bs* and YxkJ*bs* (*25*). Horizontal bars indicate putative TMSs. Arrows indicate fusion points in the chimeric proteins. Identical residues and similar residues are represented with * and ∼, respectively. Residues that are conserved in the majority of the transporters are in black boxes. (B) Topology model of the C-terminal part of CitP based on recent topology studies of CitS*kp* (*9*−*11*).

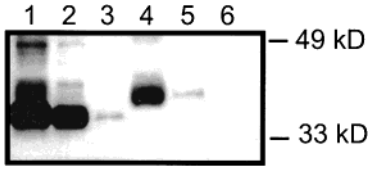

FIGURE 3: Expression levels of wild-type and chimeric transporters. Immunoblot of RSO membrane vesicles prepared from *L. lactis* NZ9000 expressing the 10-His-tagged MleP (lane 1), MC397 (lane 2), MC353 (lane 3), CitP (lane 4), CM397 (lane 5), and CM353 (lane 6). Indicated on the right are the molecular mass markers.

Expression of Wild-Type and Chimeric Transporters. The expression levels of wild-type and chimeric transport proteins in *L. lactis* NZ9000 cells were analyzed by Western blotting using antibodies raised against the His tag (Figure 3). MleP runs as a protein with an apparent molecular mass of around 35 kDa, while CitP runs at approximately 40 kDa (lanes 1 and 4). The level of expression of MleP was significantly higher than that observed for CitP. The apparent molecular masses of the chimeras correlated with the transporter that donated the N-terminal part of the sequence, i.e., the residues responsible for the different mobilities of CitP and MleP on SDS−PAGE are located in the 353 N-terminal residues. The level of expression of the chimeras was considerably lower than that observed for the wild-type proteins and dropped dramatically when the junction was more toward the N-terminus in CM353 and MC353. Again, expression levels of the chimeras seem to be related to the N-terminal sequences since the level of expression of the MC chimeras was higher than that observed for the corresponding CM chimeras (compare lanes 2 and 3 and lanes 5 and 6, respectively).

(S)-Malate Transport Activity. (*S*)-Malate is a high-affinity substrate of both CitP and MleP (*3*). The chimeric transporters were assayed for their ability to catalyze homologous (*S*)-malate counterflow and equilibrium exchange. In counterflow, right-side-out membranes prepared from cells expressing the wild-type or chimeric proteins were loaded with 5 mM (*S*)-malate and, subsequently, diluted 100-fold into buffer containing 9.8 μM ^{14}C-labeled (*S*)-malate. The gradients of labeled and unlabeled (*S*)-malate over the membrane drive the label into the lumen of the vesicles via exchange catalyzed by the transporters (*3*). The initial rates of counterflow in membranes containing wild-type CitP and MleP were very similar (Figure 4A, ● and ○). Since the membranes used in these experiments were the same as those used for the immunoblots shown in Figure 3, it follows that the specific activity of MleP is lower than the specific activity of CitP under these conditions. The initial rate of counterflow of the MC397 chimeric transporter was somewhat lower than that observed for the wild-type proteins, while the complementary CM397 transporter exhibited a ≥10-fold lower activity. These reductions correlate with the reduced level of expression of the chimeric proteins when compared to MleP and CitP. No significant counterflow activity was observed for the MC353 and CM353 proteins.

Similar observations were made for equilibrium exchange (Figure 4B). In equilibrium exchange, right-side-out membranes were loaded with 5 mM ^{14}C-labeled (*S*)-malate and,

Table 1: Affinity Constants of Wild-Type and Chimeric Transporters for External Substrates

	CitP		CM397		MleP		MC397	
	K_i (mM)	K_m (mM)	K_i (mM)	K_m (mM)	K_i (mM)	K_m (mM)	K_i (mM)	K_m (mM)
(*S*)-malate	0.068 ± 0.009	0.10 ± 0.022	0.056 ± 0.015	0.091 ± 0.022		0.47 ± 0.1		0.64 ± 0.09
citrate	0.056 ± 0.009[a]		0.042 ± 0.009		9 ± 2[a]		8.5 ± 2	
(*S*)-mandelate	>100[b]		63 ± 5		3.5 ± 0.5		13.5 ± 2	
(*S*)-2-hydroxyisovalerate	>150[b]		28 ± 4		31 ± 5		>350[b]	
(*R*)-mandelate		7 ± 2		5 ± 3	4.0 ± 0.8		4.7 ± 0.6	
(*R*)-2-hydroxyisovalerate		12.5 ± 3		3.1 ± 1.9	29 ± 9		102 ± 26	

[a] K_i value taken from ref *8*. [b] Lower limit of K_i values estimated from the inhibition at an external substrate concentration of 20 mM.

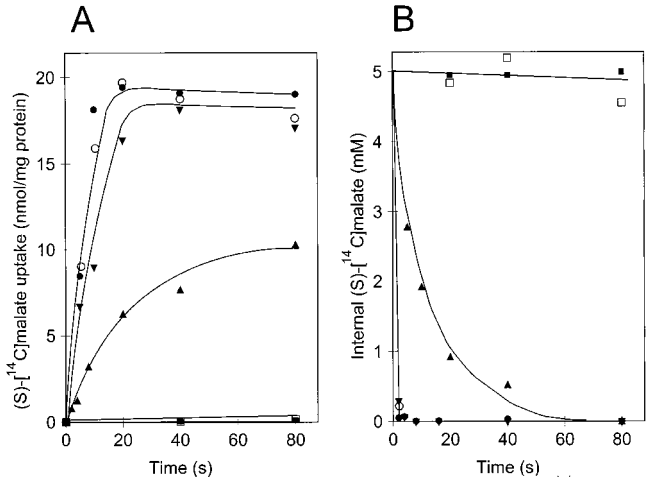

FIGURE 4: Homologous (*S*)-malate counterflow (A) and exchange (B) by wild-type and chimeric transporters. RSO membrane vesicles of *L. lactis* NZ9000 expressing CitP (●), MleP (○), CM397 (▲), MC397 (▼), CM353 (■), and MC353 (□) were preloaded with 5 mM (*S*)-malate and diluted 100-fold into buffer containing 9.8 μM (*S*)-[^{14}C]malate (A) or preloaded with 5 mM (*S*)-[^{14}C]malate and diluted 100-fold into buffer containing 5 mM (*S*)-malate (B).

subsequently, diluted 100-fold in buffer containing the same concentration of unlabeled (*S*)-malate. Exchange catalyzed by the transporters results in depletion of the radio label in the lumen of the vesicles. CitP and MleP and the MC397 chimeric protein exhibited very high and similar exchange rates, while the exchange rate of the CM397 transporter was significantly lower. No exchange activity could be detected for the MC353 and CM353 proteins.

The affinity of the transporters for external (*S*)-malate was determined by measuring the exchange and/or counterflow activity at a range of external (*S*)-malate concentrations. Since no exchange or counterflow activity was observed for CM353 and MC353, these chimeras were excluded from further studies. Under standard expression conditions, exchange and counterflow were too fast to measure initial rates in membranes containing CitP, MleP, and MC397 (see Figure 4). To allow kinetic analysis of these transporters, expression levels and thus the initial rates were reduced by manipulating the inducer concentration in the growth medium and the induction time. Affinity constants for external (*S*)-malate were found to be 0.47 and 0.084 mM for MleP and CitP, respectively (Table 1), similar to what has been reported previously for CitP and MleP without the N-terminal His tags (*8*). The affinity of CM397 for (*S*)-malate was not significantly different from the affinity of CitP, and similarly, the affinity of MC397 was very close to the affinity of MleP. In conclusion, the activities of the chimeric proteins with (*S*)-malate as the substrate correlate with the levels of expression of the proteins, and the affinities of the CM397 and MC397 chimeras appear to be determined by the N-terminal parts of the chimeras.

Specificity for Citrate. CitP translocates citrate with high efficiency, while MleP is unable to translocate citrate, but still binds citrate with low affinity (*8*). The affinity of the transporters for external citrate was measured by substituting (*S*)-malate in the dilution buffer in the exchange assay for citrate (heterologous exchange) or by assessing the inhibition of (*S*)-malate counterflow by external citrate. When corrected for the external (*S*)-malate concentration, the affinity constant for heterologous exchange and the inhibition constant for counterflow represent the same kinetic parameter (for a discussion, see ref *8*). The affinity constant of CitP for external citrate in the heterologous exchange reaction was 0.056 mM, while the inhibition constant of citrate for MleP-catalyzed counterflow was 9 mM (Table 1). Chimera CM397 effectively exchanged (*S*)-malate for citrate with an affinity constant for external citrate that was similar to that observed for CitP (Table 1). The complementary chimera MC397 was unable to translocate citrate (not shown), but citrate inhibited (*S*)-malate counterflow with an inhibition constant of 8.7 mM, as was observed for MleP. In conclusion, the structural elements enabling CitP to translocate citrate seem to be located outside the 46 C-terminal amino acids.

Specificity for Monocarboxylates. The results described above indicate that interchanging the 46 C-terminal amino acid residues of CitP and MleP altered neither the specificity nor the affinity for the di- and tricarboxylates malate and citrate. In contrast, changes in substrate specificity were observed with monocarboxylates. Mandelate is a 2-hydroxycarboxylate in which the two R groups are a hydrogen atom and a phenyl group (Figure 1). (*S*)-Mandelate at a concentration of 5 mM did not induce release of ^{14}C-labeled (*S*)-malate from right-side-out membranes containing CitP, while exchange with 5 mM (*S*)-malate was fast in the same membranes (Figure 5A). At 20 mM (*S*)-mandelate, a low-level but significant exchange was observed, indicating that CitP could translocate (*S*)-mandelate (not shown). Replacement of the 46 C-terminal amino acids with the corresponding MleP residues enabled the resulting CM397 chimera to catalyze heterologous (*S*)-mandelate−(*S*)-malate exchange at a significant rate at 5 mM (*S*)-mandelate (Figure 5B). The (*S*)-malate exchange rate was reduced due to the lower level of expression of the chimeric transporter. Clearly, the substrate selectivity of the chimeric transporter had changed. Under the same conditions, exchange rates for a number of other monocarboxylates, i.e., (*R*)-mandelate, (*S*)- and (*R*)-2-hydroxyisovalerate, and (*S*)- and (*R*)-lactate, were deter-

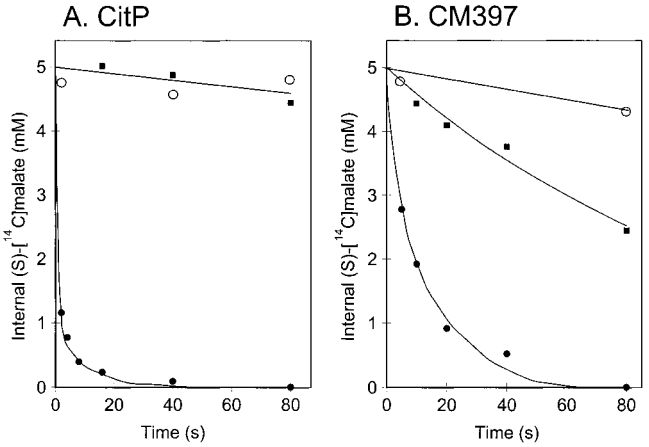

FIGURE 5: (*S*)-Mandelate−(*S*)-malate exchange catalyzed by CitP (A) and CM397 (B). RSO membrane vesicles of *L. lactis* NZ9000 expressing CitP (A) and CM397 (B) were preloaded with 5 mM (*S*)-[^{14}C]malate and diluted 100-fold into buffer containing no further additions (○), 5 mM (*S*)-malate (●), and 5 mM (*S*)-mandelate (■).

mined for CitP and CM397. The result showed a similar increase in the relative exchange rates (Figure 6A,B).

Except for (*S*)- and (*R*)-lactate, heterologous exchange with the same compounds catalyzed by MleP was much slower and significant only for the *S*-enantiomers of mandelate and 2-hydroxyisovalerate (Figure 6C,D). Heterologous lactate exchange was similar as observed for MleP without the His tag (*8*). Introducing the 46 C-terminal residues of CitP in MleP yielding MC397 resulted in the complete loss of exchange activity with these compounds; i.e., the effect was the reciprocal of what was observed with the CitP and CM397 transporters. No change in specificity for (*S*)- and (*R*)-lactate was observed for the MleP and MC397 transporters.

The changes in heterologous exchange activity of the chimeric proteins observed with the monocarboxylates reported in Figure 6 do not discriminate between changes in affinity and changes in translocation efficiency. The affinities of the transporters for the substrates were measured as discussed above for citrate. The low rate of exchange observed for (*S*)-mandelate and (*S*)-2-hydroxyisovalerate catalyzed by CitP was due to the low affinity of the transporter for these substrates. In fact, the affinity constants were too high to be measured accurately and were estimated to be >100 mM for (*S*)-mandelate and even >150 mM for (*S*)-2-hydroxyisovalerate (Table 1). In contrast, the low exchange rates with these compounds catalyzed by MleP were due to the lack of translocation; the inhibition constants for (*S*)-mandelate and (*S*)-2-hydroxyisovalerate were 3.5 and 31 mM, respectively. These results reveal an important difference between CitP and MleP; MleP binds the *S*-enantiomers of these two substrates with much higher affinity than CitP, but CitP translocates them better than MleP. A similar observation was reported before for the physiological substrate lactate (*8*). The *R*-enantiomers of mandelate and 2-hydroxyisovalerate bound with similar affinities to CitP and MleP.

The improved exchange observed for (*S*)-mandelate and (*S*)-2-hydroxyisovalerate when the 46 C-terminal residues of CitP were replaced with the corresponding residues of MleP was caused by an improved affinity of the CM397 chimera for these substrates (Table 1). The C-terminal residues of MleP seem to introduce the higher affinity of MleP for these substrates into the chimera. Most importantly, the affinity of the complementary chimera MC397 for these substrates decreased relative to the affinities of MleP for these substrates. The largest affinity changes were observed for (*S*)-2-hydroxyisovalerate for which the affinity increased by a factor of at least 5 between CitP and CM397 and decreased by a factor of at least 10 between MleP and MC397 (Figure 7). The chimeras seem to adopt the affinity for the *S*-enantiomers of mandelate and 2-hydroxyisovalerate of the transporter that donated the C-terminus.

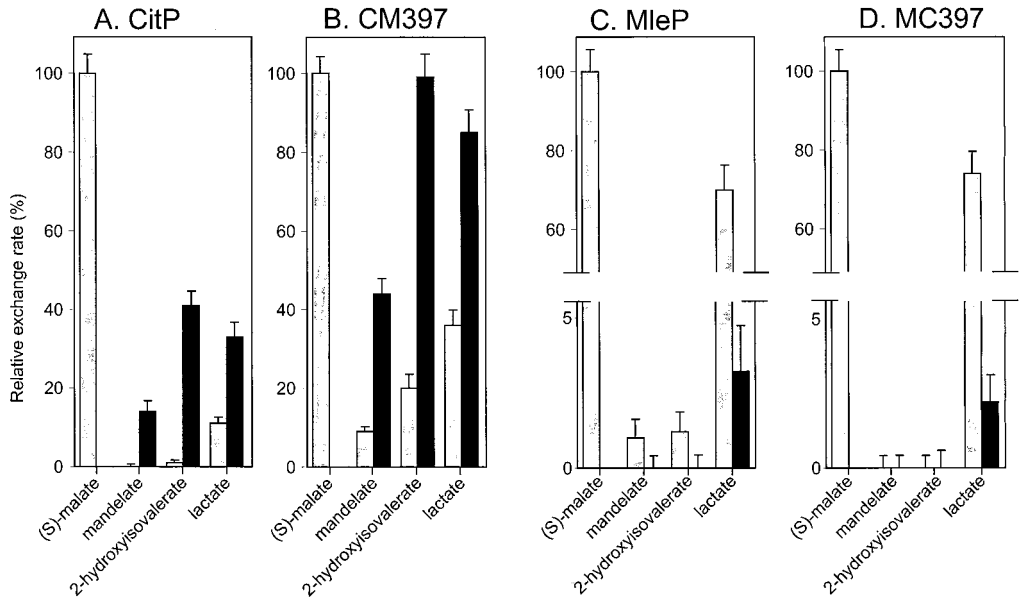

FIGURE 6: Heterologous exchange catalyzed by the wild-type and chimeric transporters. RSO membrane vesicles of *L. lactis* NZ9000 expressing CitP (A), CM397 (B), MleP (C), and MC397 (D) were preloaded with 5 mM (*S*)-[^{14}C]malate and diluted 100-fold into buffer containing the indicated substrates at 5 mM. Left (white) and right (black) bars correspond to the *S*- and *R*-enantiomeric forms of the substrates, respectively. Rates represent the average of two to four independent measurements and are given relative to the rate observed for homologous (*S*)-malate exchange. Error bars represent the standard deviations.

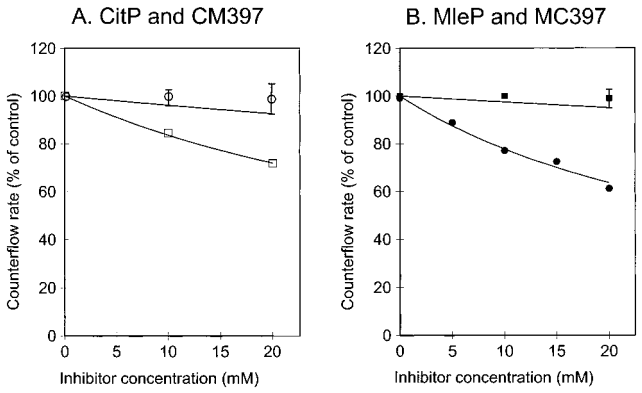

FIGURE 7: Inhibition of (*S*)-malate counterflow by (*S*)-2-hydroxyisovalerate. RSO membrane vesicles of *L. lactis* NZ9000 expressing (A) CitP (○) and CM397 (□) and (B) MleP (●) and MC397 (■) were loaded with 5 mM (*S*)-malate and diluted 100-fold in buffer containing 9.8 μM (*S*)-[^{14}C]malate and increasing concentrations of (*S*)-2-hydroxyisovalerate. Rates were indicated as the percentage of the rate observed in the absence of inhibitor. The deduced K_i values corrected for the external (*S*)-malate concentration (59.8 μM) are given in Table 1.

The observed changes in affinity between the parent and chimeric proteins were only minor for the *R*-enantiomer of mandelate, indicating that the higher heterologous exchanged rate observed for CM397 relative to that for CitP (Figure 6A,B) was mainly due to an improved translocation efficiency. In contrast, the affinities for the *R*-enantiomer of 2-hydroxyisovalerate changed 3-fold and in the opposite direction for CM397 and MC397. Replacing the C-terminal residues in CitP resulted in a increase in affinity, while replacing the same residues in MleP resulted in a decrease in affinity (Table 1).

DISCUSSION

The malate transporter MleP and the citrate transporter CitP are homologous proteins with 48% identical amino acid residues in their primary structure. Both proteins transport structurally related substrates, and differences in substrate specificity between MleP and CitP were found to be due to subtle, but well-defined, differences in binding and/or translocation properties (*8*). The conserved nature of the substrate binding site led us to believe that structural elements involved in substrate recognition might be located in conserved stretches of the amino acid residues. The highest level of sequence conservation in the 2-HCT family is found in a stretch of 46 residues at the C-terminus. To analyze the involvement of the C-terminal region in substrate recognition, we have interchanged the C-terminal stretches between the two transporters and analyzed the resulting chimeras for substrate specificity. An advantage of this approach is that the subtle differences in substrate specificity between CitP and MleP may depend on a combination of different amino acid residues at multiple positions which may be difficult to trace using site-directed mutagenesis.

Activities of the CM397 and MC397 chimeric transporters with (*S*)-malate as the substrate were lower than those observed for the wild-type transporters. The activities correlated with the reduced levels of expression of the chimeric proteins when CM397 was compared to CitP and MC397 to MleP, suggesting that the specific (*S*)-malate transport activity remained unchanged upon replacement of the C-terminal sequences. The loss of expression was dramatic when the fusion point was moved further to the N-terminus in chimeras CM353 and MC353 (Figure 3) for which no exchange activity could be detected. Similar observations were made with chimeras between CitP and MleP that had fusion points at positions 256 and 298 (not shown). The lower expression levels of CM397 and MC397 and the other chimeras seem unlikely to be due to a loss of structural integrity and, consequently, degradation of the chimeras. The chimeric molecules that enter the plasma membrane had the same kinetic parameters as the parental proteins (see below), and no breakdown products could be detected in either membrane vesicles or whole cells expressing the chimeras (not shown). Interestingly, expression levels of the wild-type transporters were also found to differ greatly even though the expression system and the induction and growth conditions were exactly the same.

CitP and MleP transport substrates that present the 2-hydroxycarboxylate motif (HO-CR_2-COO^-). Previous studies of the catalytic properties of the two transporters with a large range of 2-hydroxycarboxylates (*3*, *8*) have resulted in a model of the substrate binding site that indicates the interaction between the functional groups of the substrates and (unknown) groups on the proteins (Figure 1). In the model, two essential interactions are between groups in the binding pocket and the carboxylate and hydroxyl groups of the 2-hydroxycarboxylate motif that is common to all substrates. These interactions are like anchors that orient the substrates in the binding pocket. A third, nonessential anchoring point in the pocket (R_S side) interacts with a second carboxylate group on the substrates. This interaction is responsible for high-affinity binding of di- and tricarboxylates with a second carboxylate at R_S. (*S*)-Malate interacts with the protein via these three interactions. The kinetic parameters of chimeric proteins CM397 and MC397 with (*S*)-malate as the substrate were the same as those observed for the parental transporters that donated the N-terminal part, indicating that the spatial arrangement of the three anchoring points on the proteins was the same as in the parental proteins. The most straightforward conclusion would be that the entire binding pocket would be located in the 397 N-terminal residues; however, the possibility that part of the interacting sites in the binding pocket are conserved in the 46 C-terminal residues cannot be excluded. Clearly, the difference in the affinity of CitP and MleP for (*S*)-malate is encoded in the N-terminal part.

The citrate molecule differs from the (*S*)-malate molecule in that it has a CH_2COOH group instead of a H atom at the R_R position. This carboxylate group is protonated when the transporters interact with citrate (*8*). The CitP protein has no problem in accommodating the group and binds and transports citrate as efficiently as it does (*S*)-malate. On the other hand, MleP has a $\geq$10-fold lower affinity for citrate than for (*S*)-malate and is unable to translocate citrate. In this respect, the MC397 chimera behaved exactly like MleP and the CM397 chimera like CitP, indicating that the structural elements interacting with the CH_2COOH group of citrate at the R_R side of the binding pocket are located in the N-terminal part of the proteins.

The catalytic properties of CitP and MleP with citrate as the substrate were also recognized in the activities with monocarboxylates with a hydrophobic group at the R_R side

like (*R*)-mandelate and (*R*)-hydroxyisovalerate. Both transporters exhibited affinity for the substrates, but as was observed for citrate, MleP was found to be unable to transport them [Table 1 (*8*)]. However, unlike with citrate, replacement of the 46 C-terminal residues in the two chimeras did affect the catalytic properties with the *R*-enantiomers of the monocarboxylates. Introduction of the C-terminus of MleP in CitP yielding CM397 resulted in a higher exchange activity relative to (*S*)-malate (Figure 6). Kinetic analysis revealed that the improved activity with (*R*)-mandelate was caused by an improved translocation efficiency of CM397 relative to CitP, while in the case of (*R*)-2-hydroxyisovalerate, the affinity of the chimera improved 4-fold (Table 1). The different mechanisms suggest a different interaction of the two hydrophobic R groups with the proteins. Importantly, the affinity for (*R*)-2-hydroxyisovalerate decreased between MleP and MC397 by a factor of 3−4, showing that the results of interchanging the C-terminal sequences were reciprocal. A reciprocal effect on the translocation efficiency of (*R*)-mandelate was undetectable since MleP showed no activity with (*R*)-mandelate to begin with. In conclusion, even though the effects of interchanging the C-terminal residues on the R_R groups of the substrates are not specific and, as such, do not provide evidence for a direct interaction between the C-terminal residues and the R_R groups of the substrates, the results do indicate the involvement of the C-terminal region in catalysis.

The strongest evidence that the 46 C-terminal residues in CitP and MleP constitute part of the substrate binding pocket comes from the affinity changes observed for the *S*-enantiomers of the monocarboxylates mandelate and 2-hydroxyisovalerate that interact with the R_S side of the binding pocket. CitP has very little affinity for these substrates, but translocates them with high efficiency. In contrast, MleP binds these substrates with an affinity that is at least 1 order of magnitude higher, but translocation is very inefficient. The chimeras CM397 and MC397 adopted specifically the affinities, not the translocation efficiencies, for (*S*)-mandelate and (*S*)-hydroxyisovalerate from the parent that donated the C-terminal residues (Table 1 and Figures 6 and 7). Apparently, the C-terminal residues are involved in the initial recognition of the substrates. Consequently, at concentrations of 5 mM, heterologous exchange activity with these substrates improves considerably in CM397 and is diminished in the complementary chimera MC397. Arguments against long-range conformational effects and in favor of a model in which the 46 C-terminal residues contain the structural elements at the R_S side of the binding pocket are as follows: (i) the effects in the two chimeras are reciprocal, (ii) the chimeras adopt a property of the donor of the C-terminal sequences, and (iii) the C-terminal sequences specifically effect the affinity for the substrates.

The model for the membrane topology of CitP and MleP shows 11 putative transmembrane α-helices with the N-terminus in the cytoplasm and the C-terminus in the periplasm. The C-terminal region that in this study was interchanged between the two transporters consists of TMS XI that is outgoing and part of the cytoplasmic loop between TMSs X and XI. This study suggests that the C-terminal region interacts directly with the hydrophobic R_S groups of the monocarboxylate substrates and, thus, suggests that the binding site is at the interface of TMS XI and the other TMSs of the proteins. The hydrophobic groups at the R_S side of the binding pocket seem to interact with similar sites located on TMS XI since exchange of the C-terminal parts affects the kinetics with different substrates in a similar manner. The R_R groups of the substrates that are necessarily close in the binding pocket seem to have a less well-defined interaction with the proteins. In citrate, the polar CH_2COOH group interacts with the N-terminal TMSs while the hydrophobic R groups of (*R*)-2-hydroxyisovalerate and (*R*)-mandelate sense changes in the C-terminus, but not in the same way. This interaction of functional groups located in space at the same side of a substrate molecule with different parts of the protein is reminiscent of what has been proposed to be the mechanism by which multidrug transporter proteins interact with their substrates (*20*−*22*). No change in the three anchoring points that interact with the hydroxyl and carboxylate group of the substrate motif and the second carboxylate at R_S was observed in the chimeras, indicating that their relative localization in the binding pocket is unchanged. The anchoring points are either in the N-terminal part or conserved between CitP and MleP in the 46 C-terminal residues. The C-terminal part contains two conserved arginines, one of which is located in the TMS XI, that are good candidates for being involved in the electrostatic interactions with the carboxylate groups of the substrates. At present, we are mutating these and other residues to further analyze the role of TMS XI in substrate recognition.

ACKNOWLEDGMENT

We acknowledge D. J. Slotboom for carefully reading the manuscript and many helpful suggestions.

REFERENCES

1. Marty Teysset, C., Lolkema, J. S., Schmitt, P., Divies, C., and Konings, W. N. (1995) *J. Biol. Chem. 270*, 25370−25376.
2. Bandell, M., Lhotte, M. E., Marty Teysset, C., Veyrat, A., Prevost, H., Dartois, V., Divies, C., Konings, W. N., and Lolkema, J. S. (1998) *Appl. Environ. Microbiol. 64*, 1594−1600.
3. Bandell, M., Ansanay, V., Rachidi, N., Dequin, S., and Lolkema, J. S. (1997) *J. Biol. Chem. 272*, 18140−18146.
4. Poolman, B., Molenaar, D., Smid, E. J., Ubbink, T., Abee, T., Renault, P. P., and Konings, W. N. (1991) *J. Bacteriol. 173*, 6030−6037.
5. Lolkema, J. S., Poolman, B., and Konings, W. N. (1996) in *Handbook of Biological Physics* (Konings, W. N., Kaback, H. R., and Lolkema, J. S., Eds.) pp 229−260, Elsevier, Amsterdam.
6. Marty Teysset, C., Posthuma, C., Lolkema, J. S., Schmitt, P., Divies, C., and Konings, W. N. (1996) *J. Bacteriol. 178*, 2178−2185.
7. Magni, C., de Mendoza, D., Konings, W. N., and Lolkema, J. S. (1999) *J. Bacteriol. 181*.
8. Bandell, M., and Lolkema, J. S. (1999) *Biochemistry 38*, 10352−10360.
9. van Geest, M., and Lolkema, J. S. (1999) *J. Biol. Chem. 274*, 29705−29711.
10. van Geest, M., Nilsson, I., von Heijne, G., and Lolkema, J. S. (1999) *J. Biol. Chem. 274*, 2816−2823.
11. van Geest, M., and Lolkema, J. S. (2000) *Biochim. Biophys. Acta 1466*, 328−338.

12. de Ruyter, P. G., Kuipers, O. P., and De Vos, W. M. (1996) *Appl. Environ. Microbiol. 62*, 3662−3667.
13. Kuipers, O. P., Beerthuyzen, M. M., Siezen, R. J., and De Vos, W. M. (1993) *Eur. J. Biochem. 216*, 281−291.
14. Putman, M., van Veen, H. W., Poolman, B., and Konings, W. N. (1999) *Biochemistry 38*, 1002−1008.
15. Sambrook, J., Fritsch, E. F., and Maniatis, T. (1989) *Molecular Cloning: A Laboratory Manual*, Cold Spring Harbor Laboratory Press, Cold Spring Harbor, NY.
16. Holo, H., and Nes, I. F. (1989) *Appl. Environ. Microbiol. 55*, 3119−3123.
17. Gaillard, I., Slotboom, D. J., Knol, J., Lolkema, J. S., and Konings, W. N. (1996) *Biochemistry 35*, 6150−6156.
18. Horton, R. M., Hunt, H. D., Ho, S. N., Pullen, J. K., and Pease, L. R. (1989) *Gene 77*, 61−68.
19. Lowry, O. H., Rosebrough, N. J., Farr, A. L., and Randall, R. J. (1951) *J. Biol. Chem. 193*, 265−275.
20. Zheleznova, E. E., Markham, I., Edgar, I., Bibi, I., Neyfakh, A. A., and Brennan, R. G. (2000) *Trends Biochem. Sci. 25*, 39−43.
21. Zheleznova, E. E., Markham, P. N., Neyfakh, A. A., and Brennan, R. G. (1999) *Cell 96*, 353−362.
22. Vazquez-Laslop, N., Markham, P. N., and Neyfakh, A. A. (1999) *Biochemistry 38*, 16925−16931.
23. van der Rest, M. E., Siewe, R. M., Abee, T., Schwarz, E., Oesterhelt, D., and Konings, W. N. (1992) *J. Biol. Chem. 267*, 8971−8976.
24. Kawai, S., Suzuki, H., Yamamoto, K., and Kumagai, H. (1997) *J. Bacteriol. 179*, 4056−4060.
25. Kunst, F., Ogasawara, N., Moszer, I., et al. (1997) *Nature 390*, 249−256.

BI0011882